

Simulating and Measuring the Acoustic Radiation Force of a Focused Ultrasonic Beam on Elastic Spheres in Water

A. V. Nikolaeva^a, *, M. M. Karzova^a, S. A. Tsysar^a, V. A. Khokhlova^a, and O. A. Sapozhnikov^a

^a*Faculty of Physics, Moscow State University, Moscow, 119991 Russia*

**e-mail: av.nikolaeva@physics.msu.ru*

Abstract—The phenomenon of acoustic radiation force acting on solid spherical scatterers inside the field of a focused ultrasonic beam is experimentally studied. Nylon and glass beads are used as scatterers; the acoustic field is generated by a piezoceramic transducer of the megahertz frequency range in water. The angular spectrum of the ultrasonic beam, obtained from the measured transverse distribution of the amplitude and phase of the acoustic pressure, is used to calculate the theoretical value of the radiation force. The results from these calculations are in agreement with the experimentally determined value of the radiation force.

DOI: 10.3103/S1062873819010192

INTRODUCTION

A promising application of acoustic beams exerting force on irradiated objects is the recently proposed noninvasive propulsion of kidney stones by means of radiation force [1–3]. This approach is one basis of the promising noninvasive and low-invasive treatment of urolithiasis in its early stages, which reduces the probability of a recurrence after shock-wave lithotripsy and obviates the need for surgical intervention. It can also be applied in case of occlusion of the ureteral orifice by a large stone, in order to push the stone back to the kidneys' collecting system when it is necessary to stop renal colic and prevent an emergency operation.

The possibility of using the radiation force of an ultrasonic beam to push nephroliths has been demonstrated in model experiments on a phantom kidney [1] and in in vivo experiments on pigs [2]. In addition, more than ten volunteer patients with the motion of stones registered in their kidneys recently underwent trial treatment with the action of an acoustic field force [3]. The stones were pushed by standard diagnostic ultrasonic transducers operating not in the conventional regime of visualization but in that of long-pulse ultrasonic emission. Steady motion of stones with sizes of 2–7 mm was observed at the maximum possible diagnostic power of the transducer. Despite the success in moving fragments of different sizes in the kidneys, the problem of measuring the radiation force and the direction of its action with greater precision has yet to be thoroughly studied. To introduce this procedure into clinical practice, we must develop a numerical model and make highly precise experi-

mental measurements of the radiation force in the field of an arbitrary beam.

Focused beams generated by transducers of different types are used in practice. In this work, we propose an experimental setup designed to measure the radiation force acting on elastic spherical scatterers several mm in size and made of different materials. The corresponding numerical calculations of the force for the considered scatterers are performed on the basis of the measured two-dimensional distribution of the amplitude and phase of acoustic pressure in the beam cross section (acoustic hologram).

EXPERIMENTAL

In this work, we investigated the impact of a focused ultrasonic beam on elastic spherical scatterers. A single-element focused transducer in a shape of a spherical cup with focal distance $F = 7$ cm, aperture radius $r = 5$ cm, and operating frequency $f = 1.072$ MHz was the source of acoustic field. The transducer operated in the continuous harmonic wave mode.

Elastic beads 2–3 mm in size and made of nylon and glass were chosen as scatterers. The corresponding elastic characteristics were the following: For nylon, density ρ_s was 1125 kg m^{-3} , and the velocities of longitudinal c_l and shear (transverse) c_t waves were 2620 and 1080 m s^{-1} , respectively. For glass, $\rho_s = 2500 \text{ kg m}^{-3}$; $c_l = 5920 \text{ m s}^{-1}$; and $c_t = 3420 \text{ m s}^{-1}$. Our experimental investigations were performed for two nylon beads with radii $a = 2$ mm and $a = 3$ mm, and one glass bead with $a = 2$ mm.

ANALYTICAL RELATIONSHIP BETWEEN THE RADIATION FORCE AND FIELD STRUCTURE

Our numerical calculations of the radiation force exerted by the ultrasonic beam on an elastic bead was based on the theoretical approach described in [4]. In this work, we present only the main relations. For a spherical scatterer in an ideal liquid, the component of the radiation force directed along the z -axis of beam propagation was calculated numerically:

$$F_z = -\frac{1}{4\pi^2 \rho c^2 k^2} \operatorname{Re} \left\{ \sum_{n=0}^{\infty} \Psi_n \sum_{m=-n}^n B_{nm} H_{nm} H_{n+1,m}^* \right\}. \quad (1)$$

Here, c is the speed of sound in the liquid; $k = 2\pi f/c$ is the wave number; ρ is the density of the surrounding liquid; $Y_{nm}^*(\theta_k, \varphi_k)$ represents the complex conjugate spherical harmonics; and index Re denotes the real part of the quantity in the curly brackets. Coefficients $B_{nm} = \sqrt{(n+m+1)(n-m+1)/(2n+1)(2n+3)}$, $H_{nm} = \int_{k_x^2+k_y^2 < k^2} dk_x dk_y S(k_x, k_y) Y_{nm}^*(\theta_k, \varphi_k)$ describe the structure of the incident field defined by angular spectrum $S(k_x, k_y)$. Functions Ψ_n are determined by the properties of the scatterer and medium. They characterize the scattering of plane waves on the elastic sphere with the radius a : $\Psi_n = \Psi_n\{ka, k_1 a, k_t a, \rho, \rho_s\}$. Here, $k_1 = \omega/c_1$, $k_t = \omega/c_t$. Functions Ψ_n were described more in detail in [4, 5].

If a scatterer is inside the field of an axially symmetric beam at its axis, relation (1) is sufficient to calculate the desired radiation force, since its value is in this case $F = F_z$, and the transverse components of the force are equal to zero: $F_x = F_y = 0$. In the general case of a nonsymmetric beam or a scatterer off the axis, the radiation force has three non-zero components. Relations similar to (1) for the other two components can be also calculated using the angular spectrum [4]. In this work, numerical and experimental calculations of the radiation force were performed only for the axis of a focused beam; relation (1) was in this case sufficient for the calculations.

According to expression (1), in order to calculate numerically the radiation force we need to know the angular spectrum of the power beam. It can be found using the known distribution of the complex amplitude of the acoustic pressure P , defined along some plane $(x, y, z = z_0)$ as

$$S(k_x, k_y) = e^{-iz_0 \sqrt{k^2 - k_x^2 - k_y^2}} \times \int_{-\infty}^{+\infty} \int_{-\infty}^{+\infty} dx dy P(x, y, z_0) e^{-i(k_x x + k_y y)}. \quad (2)$$

In theory, the angular spectrum of the field of a single-element transducer in the shape of a spherical cup

can be calculated by assuming the transducer surface oscillates in a manner similar to that of piston-type sound sources. In this case, the incident field can be obtained using the Rayleigh integral [6]. However, more accurate calculations require an approach in which the angular spectrum is found by considering the real field structure and character of oscillations of the transducer plate. One such approach that allows us to characterize the fields with a high degree of precision is acoustic holography [7]. Based on measurements of two-dimensional distribution $P(x, y, z_0)$ of the amplitude and phase of acoustic pressure in the beam cross section (an acoustic hologram), we can calculate angular spectrum (2) and reconstruct the entire transducer field at some distance from the transducer's surface [7]:

$$P(x, y, z) = \frac{1}{4\pi^2} \times \int_{-\infty}^{\infty} \int_{-\infty}^{\infty} S(k_x, k_y) e^{ik_x x + ik_y y + i\sqrt{k^2 - k_x^2 - k_y^2} z} dk_x dk_y. \quad (3)$$

Once the angular spectrum is known, we can also calculate the total acoustic power of the beam [4]:

$$W = \frac{1}{8\pi^2 \rho c} \iint_{k_x^2 + k_y^2 \leq k^2} \sqrt{1 - \frac{k_x^2 + k_y^2}{k^2}} |S(k_x, k_y)|^2 dk_x dk_y. \quad (4)$$

In solving radiation force problems, it is convenient to use parameter $Y = Fc/W$, normalized by the power and speed of sound. Relations (1)–(4) completely determine numerical calculations of the dimensionless parameter $Y_z = F_z c/W$ for the axial component of the radiation force on the beam axis, which is in turn needed to be compared with the results of the radiation force measurements.

ACOUSTIC FIELD STRUCTURE MEASUREMENTS

Following the procedure described above, we measured acoustic hologram $P(x, y, z_0)$ (amplitude and phase) of the power transducer at a distance of $z_0 = 55$ mm from the transducer's surface (Fig. 1a). The measurements were performed by an ONDA HNA 0400 needle hydrophone. Voltage amplitude U measured at the hydrophone output was recalculated to the corresponding acoustic field pressure according to hydrophone sensitivity $G = 0.75$ V MPa⁻¹, determined experimentally by acoustic beam weighing [7]. Figure 1b shows the distribution of angular spectrum modulus $S(k_x, k_y)$ obtained according to formula (2), and the corresponding transducer field calculated using formula (3) in transverse plane xz . It should be noted that the acoustic field can, with good approximation, be considered axially symmetric. The focus is located at a distance of $z = 70$ mm from the transducer's surface,

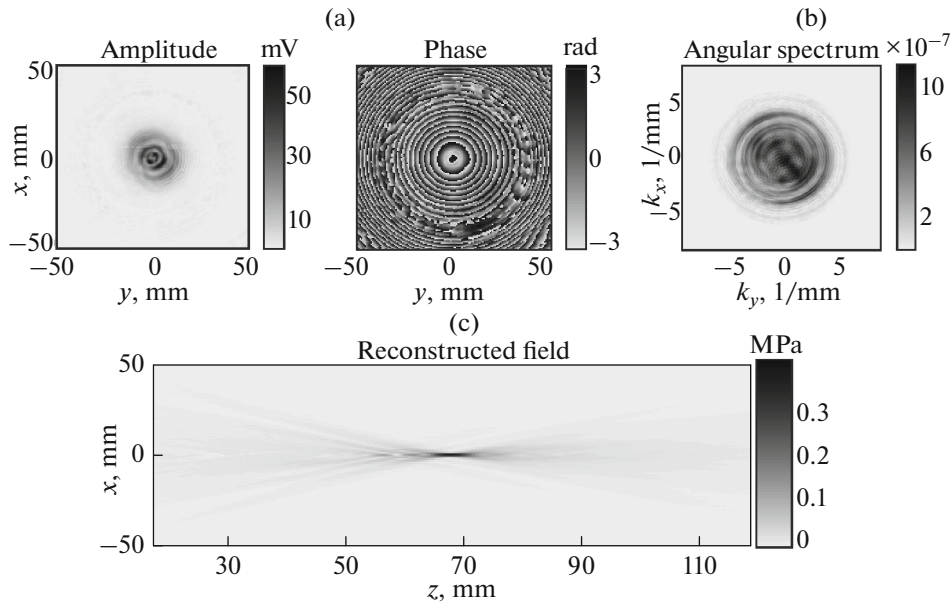


Fig. 1. (a) Measured field amplitude and phase in the transverse plane of a transducer at 120×120 points with a spacing of 0.5 mm; (b) reconstructed angular spectrum of the transducer; (c) pressure field of the focused beam in the plane.

as it should be. The half-amplitude diameters of the focal spot are 2 mm in the transverse direction and 7 mm in the longitudinal direction.

RADIATION FORCE MEASUREMENTS

The radiation force was measured using a specially designed experimental setup (Fig. 2). The focused source was located on the bottom of a tank with degassed water.

Scatterers in the shape of elastic beads were arranged in the transducer field in a specially designed mount consisting of three levels of parallel, tautly-drawn thin fishing lines with a diameter of $d = 0.08$ mm. The mount could be moved in three orthogonal directions with steps of up to 0.1 mm using a positioning system. The three-level system of fishing lines was needed to provide a number of functions. The first level was the support for the bead; the second level was needed to limit the sideways motion of the scatterer (the supporting lines of second level were stretched wider than other levels); and the third level limited the upward motion of the bead subjected to the radiation force.

A thin, acoustically transparent film was placed directly in front of the scatterer to eliminate hydrodynamic flows of the liquid caused by the acoustic beam (acoustic streaming). To minimize the impact of the waves reflected from the upper water–air boundary on the scatterer, a rubber absorber with a diameter of $d = 100$ mm was arranged along the path of beam propagation near the water’s surface.

Measurements were performed along the transducer’s axis with steps of 0.2 mm. The motion of the scatterer caused by the radiation force was observed using a camcorder aimed through an inspection notch in the mount.

Dimensionless radiation force Y_z was determined at each point by measuring the threshold field power corresponding to the moment when the axial component of the radiation force acting on the scatterer with volume V in the liquid with density ρ compensated by the forces of gravity and buoyancy:

$$F_z = F_{\text{thresh}} = gV(\rho_s - \rho). \quad (5)$$

At each point, threshold value F_z was attained at the corresponding level of acoustic power W , which was in

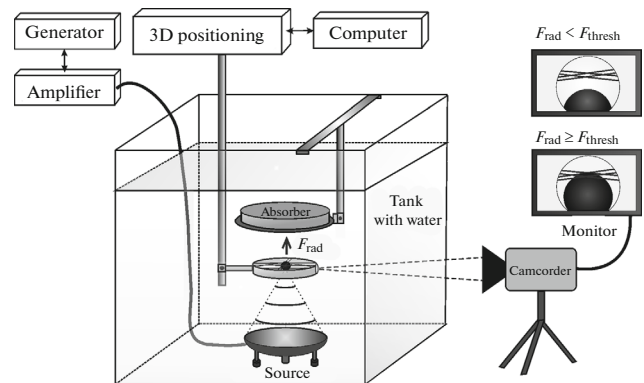


Fig. 2. Experimental setup for measuring the radiation force acting on elastic spherical scatterers.

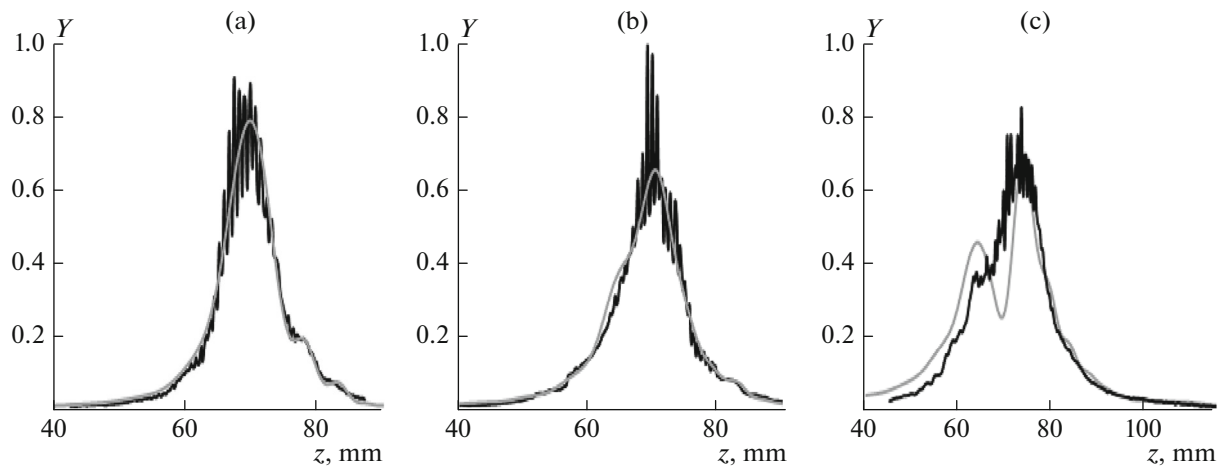


Fig. 3. Numerical curves (grey) and experimental results (black) from measuring the radiation force for three scatterers: (a) glass, $r = 2$ mm; (b) nylon, $r = 2$ mm; (c) nylon, $r = 3$ mm.

turn determined by the voltage applied from the Agilent 33250A signal generator through the E&I RF Power Amplifier. We used the following algorithm to determine the threshold value of the voltage at the generator: at the first stage, a fortiori high voltage was applied to the transducer so that the scatterer would detach from the lower supporting lines and rest on the upper lines. Gradually reducing the voltage, we then registered the moment at which the scatterer detached from the upper fishing lines, which corresponded to the threshold value U_{thres} . The voltage at the generator was recalculated to the corresponding acoustic power with allowance for signal gain and the efficiency with which electric power was transformed into acoustic power.

RESULTS AND DISCUSSION

The results from our experimental measurements of the radiation force acting on scatterers made from nylon and glass are presented in Fig. 3, along with the corresponding results from numerical calculations.

Each of the three graphs corresponds to the material and size of the scatterer: grey curves indicate numerical calculations; black curves correspond to measurement results. It should be noted that for all three scatterers, the numerical and experimental results in the region behind the focus are in agreement with an error of up to 8%. For the scatterers with a radius of $r = 2$ mm, the results also coincide with a high level of accuracy in the prefocal region (Figs. 3a, 3b). Poorer agreement (error, 20–25%) between the numerical calculations and experimental data in the prefocal region is observed for the nylon bead with a radius of $r = 3$ mm. We observe oscillations for all scatterers in the focal region, due to the generation of standing waves

between the transducer's surface and each scatterer. Despite the influence of the standing waves, the general trend of the experimental curves is similar to that of the numerical results.

Let us also note an interesting effect observed for the nylon scatterer with a radius of $r = 3$ mm (Fig. 3c). Here, as distinct from the beads with a radius of $r = 2$ mm, the radiation force maximum at the transducer axis is reached not at the beam focus but at some distance from it, in the region where the beam radius approaches the size of the scatterer. For the scatterers with $r = 2$ mm, the width of the focused beam at the focus is close to the size of the scatterer, which corresponds to the maximum value of the radiation force along the transducer axis. This effect is associated with the generation of shear waves in the scatterer and a more efficient transfer of the beam's momentum to the scattering object. This was discussed more in detail in [8, 9].

CONCLUSIONS

The measuring technique proposed in this work allows us to determine with a high degree of accuracy the value of the radiation force acting on spherical scatterers, as was confirmed by the numerical results obtained by considering the real structure of our acoustic beam.

ACKNOWLEDGMENTS

This work was supported by the Russian Foundation for Basic Research, project nos. 17-02-00261, 18-02-00991, and 18-32-00659; and by RF Presidential Grant SP-2621.2016.4 (M.M. Karzova).

REFERENCES

1. Shah, A., Owen, N., Lu, W., et al., *Urol. Res.*, 2010, vol. 38, no. 6, p. 491.
2. Shah, A., Harper, J.D., Lu, W., et al., *J. Urol.*, 2012, vol. 187, no. 2, p. 739.
3. May, P.C., Bailey, M.R., and Harper, J.D., *Curr. Opin. Urol.*, 2016, vol. 26, no. 3, p. 264.
4. Sapozhnikov, O.A. and Bailey, M.R., *J. Acoust. Soc. Am.*, 2013, vol. 133, no. 2, p. 661.
5. Hasegawa, T., Ochi, M., and Matsuzawa, K., *J. Acoust. Soc. Am.*, 1981, vol. 69, no. 4, p. 937.
6. Sapozhnikov, O.A. and Sinilo, T.V., *Akust. Zh.*, 2002, vol. 48, no. 6, p. 813.
7. Tsysar, S., Sapozhnikov, O., and Kreider, W., *Proc. Meet. Acoust.*, 2013, vol. 19, p. 055015.
8. Nikolaeva, A.V. and Sapozhnikov, O.A., *Bull. Russ. Acad. Sci.: Phys.*, 2017, vol. 81, no. 1, p. 80.
9. Cleveland, R.O. and Sapozhnikov, O.A., *J. Acoust. Soc. Am.*, 2005, vol. 118, no. 4, p. 2667.

Translated by E. Smirnova